CHEMISTRY OF MATERIALS

Article

pubs.acs.org/cm

Phase Behavior in the $LiBH_4$–LiBr System and Structure of the Anion-Stabilized Fast Ionic, High Temperature Phase

Irene Cascallana-Matias,[†,‡] David A. Keen,[§] Edmund J. Cussen,[*,‡] and Duncan H. Gregory[*,†]

[†]WestCHEM, School of Chemistry, Joseph Black Building, University of Glasgow, Glasgow G12 8QQ, United Kingdom

[‡]WestCHEM, Department of Pure and Applied Chemistry, University of Strathclyde, Glasgow G1 1XL, United Kingdom

[§]ISIS Facility, Rutherford Appleton Laboratory, Harwell Oxford, Didcot, Oxfordshire OX11 0QX, United Kingdom

Supporting Information

ABSTRACT: The fast ionic, high temperature (HT) phase of $LiBH_4$ can be stabilized by Br^- substitution. Lithium borohydride bromide compounds, $Li(BH_4)_{1-x}Br_x$, have been synthesized mechanochemically, with and without thermal treatment and the resulting phase behavior determined as a function of composition. Single phase materials exist for $0.29 \leq x \leq 0.50$ with conductivity 2 orders of magnitude higher than $LiBH_4$ at 313 K. Powder neutron diffraction has been used to resolve the details of the crystal structure of one such compound. These demonstrate that $^7Li(^{11}BD_4)_{0.667}Br_{0.333}$ retains the HT structure (hexagonal space group $P6_3mc$, $a \approx 4.2$ Å, $c \approx 6.7$ Å) from 293 to 573 K. The borohydride bromide exhibits considerable static and dynamic disorder, the latter invoking complex rotational motion of the $(BH_4)^-$ anions.

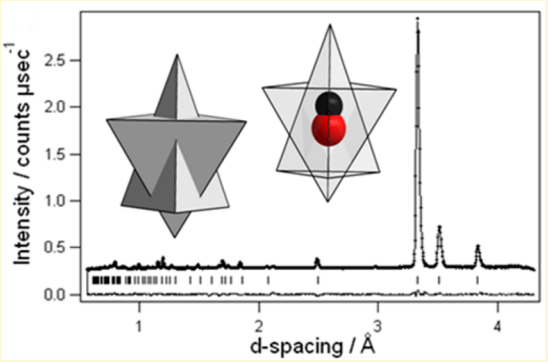

INTRODUCTION

The decomposition and release of hydrogen from a number of complex hydrides such as lithium borohydride is linked to a transition to a fast lithium ion conducting state.[1,2] At room temperature $LiBH_4$ crystallizes with an orthorhombic (LT) structure and at 383 K undergoes a phase transition to a hexagonal (HT) phase that exhibits fast lithium ion conductivity, with values of up to 10^{-2} S cm^{-1}.[1] The structure of the LT phase has been thoroughly examined and can be described as a distorted variant of the wurtzite structure with the Li^+ cations occupying the four-coordinate tetrahedral sites between hexagonally stacked layers of BH_4^-.[3] The distortion to orthorhombic symmetry allows buckling of the anion layers and ordering of the slightly distorted tetrahedral anions. The structure of the HT phase contains considerable disorder in the anion orientation and has been the subject of experimental and theoretical studies.[4−6] Several results and interpretations have been advanced to explain the behavior of the BH_4^- units in the fast Li^+ conducting material. Various degrees of dynamic orientational disorder have been proposed from the threefold rotation of BH_4 about a single B−H bond (possibly combined with occasional exchange between rotationally disordered H atoms and the fixed H atom) to unconstrained, free rotation of all H atoms to give an effectively spherical anion.[2,7,8] Attempts have been made to stabilize the hexagonal phase at room temperature using anion substitution. Partial anion replacement effected by mechanical and thermal reaction with appropriate halides leads to the formation of the hexagonal structure analogous to the HT phase of $LiBH_4$.[9−11] However, the HT form has never been isolated at room temperature as a single phase with bromide. Here we show that two preparative methods can produce phase pure samples of the fast ion conductive phase with controlled molar ratios $0.29 \leq x \leq 0.50$ in the series $Li(BH_4)_{1-x}Br_x$. These materials have been obtained by either extensively mechanically milling a mixture of $LiBH_4$ and LiBr or by combining a shortened milling with thermal treatment. The resultant materials have been characterized by both powder X-ray and powder neutron diffraction, thermal analysis, transport measurements, and electron microscopy. We have used these data to compile a phase diagram for the full compositional series $Li(BH_4)_{1-x}Br_x$, and we report these results together with a detailed structural model of the orientational disorder of the BH_4 anion in the fast Li^+ conducting hexagonal phase.

EXPERIMENTAL SECTION

Synthesis. All manipulations were performed in a nitrogen-filled or argon-filled glovebox (<5 ppm of O_2; < 10 ppm of H_2O). Anhydrous $LiBH_4$ (Sigma-Aldrich, ≥ 95%) and LiBr (Sigma-Aldrich, ≥ 99%) were obtained commercially and used directly without further purification. Approximately 0.5 g of $LiBH_4$–LiBr mixtures were mechanically milled under a nitrogen atmosphere using a Retsch PM100 ball mill. The ball milling was performed in periods of 2 min of milling interspersed by 2 min breaks to minimize heating of the samples. The sample to ball ratio was 1:40 and both the vial and 10 mm diameter balls were made from stainless steel. The agitation frequency was 500 rpm.

Received: September 17, 2015
Revised: October 26, 2015
Published: October 26, 2015

DOI: 10.1021/acs.chemmater.5b03642
Chem. Mater. 2015, 27, 7780−7787

The materials were prepared by two different routes: (a) by mechanochemical milling for 24 h or (b) milling for 4 h followed by heating the milled mixtures to 573 K for 5−24 h. The longer annealing times were necessary to give a single phase product for higher bromide concentrations (Table S1).

The sample for the neutron scattering experiment was isotopically enriched with D, ^{7}Li and ^{11}B to avoid problems with neutron incoherent scattering and absorption. Anhydrous $^{7}Li^{11}BD_4$ (Katchem, > 99.8% ^{7}Li, > 99.8% ^{11}B, > 98% D) and LiBr (Sigma−Aldrich, ≥ 99%) were obtained commercially and used directly without further purification. The samples (1.0 g) were prepared by ball milling and thermal heating with longer heating times being necessary due to the larger quantity of material being prepared. Since the sample is air-sensitive, it was loaded into a sealed vanadium can in an inert atmosphere glovebox before the experiment.

Characterization. Powder X-ray diffraction (PXD) was used to identify the reaction products and characterize their respective structures. PXD experiments were conducted with a Bruker D8 Advance powder diffractometer operating with Cu Kα radiation in transmission geometry with samples mounted in spinning sealed capillaries. Diffraction data for phase identification were typically collected over $5° \leq 2\theta \leq 85°$ with a 0.017° step size and scan times of 1 h and over $5° \leq 2\theta \leq 95°$ for 12 h for structural analysis. Raman data were collected at room temperature using a Horiba Jobin Yvon system with a 532 nm green laser. A hole aperture of 50 μm, 100 g mm^{-1} grating, and a synapse CCD detector were employed. Sealed glass capillaries were used to contain samples and thereby prevent air/moisture exposure during spectroscopic analysis.

Thermogravimetric−differential thermal analysis−mass spectrometry (TG-DTA-MS) experiments were conducted under flowing argon (99.998%, BOC) in a Netzsch 409 PC STA Instruments coupled to a Hiden Analytical HPR 20 mass spectrometer at a heating rate of 4 K min^{-1}. The STA Instruments was located in an argon-filled glovebox (O_2, H_2O < 0.5 ppm, UNILab, MBraun) where samples (≈10 mg) were loaded in high-walled Al_2O_3 pans. Sample morphology and composition were studied using SEM (XL 30 ESEM, Philips, 25 kV accelerating voltage). An Oxford Instruments X-act spectrometer was coupled to this microscope for EDX analysis. The instrument is calibrated using the INCA EDX analysis software (Cu used for all calibration measurements), and the software also allows selection of regions for analysis and definition of measurement parameters.

Electrochemical impedance measurements were performed on cylindrical sample pellets of 13 mm diameter and 1−2 mm thickness that had been formed by pressing at room temperature under a load of 1 tonne for 20 min. A platinum paste was applied to opposite faces of the pellet to make electrical contacts. Data were collected on heating, and the temperature of the system was allowed to equilibrate for at least 1 h before every data collection. Data were collected using a Solartron 1260 impedance analyzer and were analyzed using equivalent circuit analysis as implemented in the ZView2 software package.

Time-of-flight powder neutron diffraction (PND) data were collected between 293 and 573 K using the General Materials diffractometer, GEM, at the ISIS neutron source at the Rutherford Appleton Laboratory in Oxfordshire.[12] Samples were contained in vanadium cans with a diameter of 6 mm. Using standard procedure, the data from each of the instrument's detector banks were corrected for absorption, normalized to account for the incident neutron spectrum and detector efficiencies and summed.[12] The data were analyzed using Rietveld refinement as implemented in the GSAS software package[13] via the EXPGUI interface[14] against multiple data sets.

RESULTS AND DISCUSSION

Reactivity and Preparation. Combinations of mechanical and thermal treatments have been used in borohydride−halide systems before, and various techniques were employed to investigate the roles of these two processes in the reactions.[10,15,16,10,17] Raman spectroscopy is sensitive to the orthorhombic to hexagonal transition in $LiBH_4$ via the characteristic B−H bending mode splitting at ν_2 = 1282 cm^{-1} and ν_2' = 1297 cm^{-1} in the lower symmetry structure.[3,18−20] Data from our bromide-doped samples show that the orthorhombic symmetry has been eliminated in $Li(BH_4)_{0.667}Br_{0.333}$ indicating that the reaction has stabilized the high temperature structure of $LiBH_4$ (Figure S1). Examination of the samples using scanning electron microscopy reveals particle morphologies that bear little resemblance to those of either of the reagents. $Li(BH_4)_{0.667}Br_{0.333}$ can be prepared either by (1) extensive milling or (2) by a reduced period of milling followed by thermal treatment (at 573 K). Micrographs from samples prepared via these two routes revealed that milling only leads to well-defined petal-like structures agglomerated into discrete, relatively uniform and almost spherical aggregates. Each sphere is of the order of 50 μm in diameter. The effect of thermal treatment is to give more homogeneous, dispersed particles as shown in Figure 1.

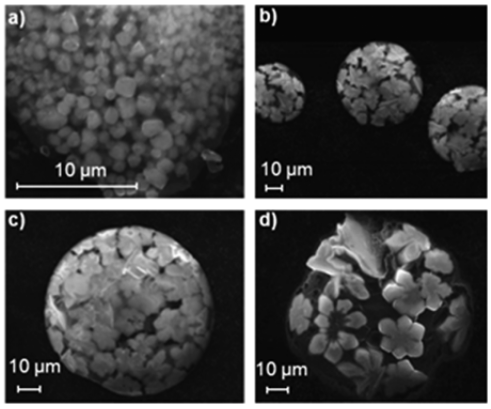

Figure 1. SEM images from $Li(BH_4)_{0.667}Br_{0.333}$ prepared by (a) milling and thermal treatment; (b), (c), and (d) milling only.

The effect of the thermal treatment is further understood by examining TG-DTA data from $Li(BH_4)_{0.667}Br_{0.333}$ (Figure 2)

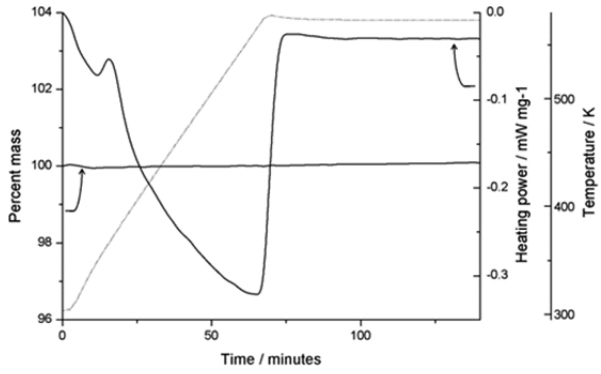

Figure 2. TG-DTA profile of milled $Li(BH_4)_{0.667}Br_{0.333}$ on heating from room temperature to 573 K. The temperature is indicated by the dashed line.

that had been milled for 4 h only (i.e., prior to the heat treatment part of the synthesis process). DTA data show one endothermic event at 368(1) K and no other higher temperature features while the TG profile demonstrates that no mass loss occurs from room temperature to 573 K. The endothermic event corresponds to the orthorhombic−hexago-

DOI: 10.1021/acs.chemmater.5b03642
Chem. Mater. 2015, 27, 7780−7787

nal phase transition with a reduction in transition temperature from that observed in pure LT−$LiBH_4$ (383 K).[1,21] Further, unlike pure $LiBH_4$ (MP 541 K)[22] there is no evidence of a melting transition (or decomposition) below 573 K.

PXD was used to characterize the materials prepared by both the extended milling and milling/heating routes. Inspection of the diffraction patterns collected from samples across the compositional series showed that all Bragg peaks could be indexed to one of three phases (Figure 3, Table S3, Figures S4 and S5). In composition region I, for the most $(BH_4)^-$-rich compositions ($0 \leq x < 0.20$), an orthorhombic (LT $LiBH_4$-type) phase is observed with a progressive contraction of the unit cell with increasing Br^- content. From $x = 0.20$ a second, hexagonal (HT $LiBH_4$-type) phase coexists with the orthorhombic material (region II). Although the cell volume of the orthorhombic phase in region II was observed to continue to decrease with increasing x, the weak, broad reflections were not sufficient to allow structure refinement (and hence the points are not indicated in Figure 3). With further increasing Br^- content the orthorhombic phase is eliminated to give single-phase hexagonal HT $LiBH_4$-type samples in the range $0.29 \leq x \leq 0.50$ (region III). For $x \geq 0.67$ a cubic (rock salt) phase is apparent within a two phase hexagonal/cubic region existing over at least $0.67 \leq x \leq 0.75$ (region IV). Finally region V contains the single cubic rock salt phase of LiBr. Although from the compositions discovered in region IV, we know that LiBr is not a line phase, the precise position of the phase boundary (IV−V) is yet to be determined. For each of the orthorhombic, hexagonal, and cubic phases (regions I, III, V) there is a progressive decrease in the cell volume as the Br^- content is increased.

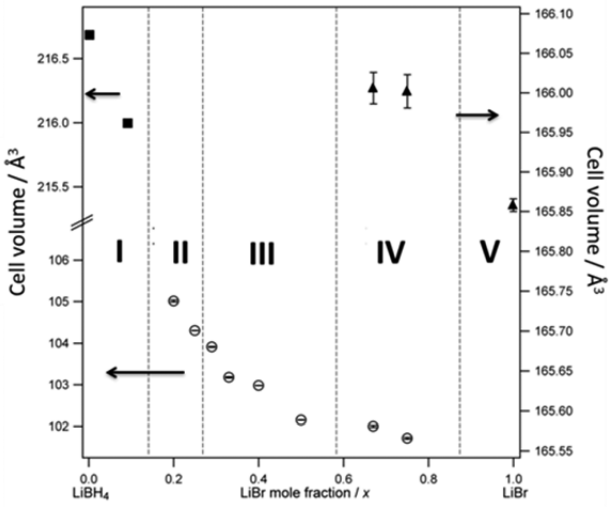

Figure 3. Structure field map manifested as the respective unit cell volumes as a function of LiBr mole fraction in $Li(BH_4)_{1-x}Br_x$. I−V represent the distinct phase regions within compositional space. Black squares denote the LT orthorhombic $LiBH_4$ structure (top-left y axis); open circles denote the HT hexagonal $LiBH_4$ structure (bottom-left y axis); black triangles denote the cubic LiBr (NaCl-type) structure (right y axis).

Ion Transport Properties. Impedance data analyzed in the complex plane showed the semicircle at high frequencies and the linear response at low frequencies characteristic of ionic conductivity and ion blocking electrodes. At the lower temperatures two semicircles were observed, suggesting intra- and intergrain transport could be resolved. However, the high frequency semicircle moved out of the measurement range at higher temperatures, and so the data were analyzed using an equivalent electrical circuit to extract the values for the total resistivity of the material (Figures S2 and S3). As shown in Figure 4, the mixed borohydrides demonstrate conductivities of

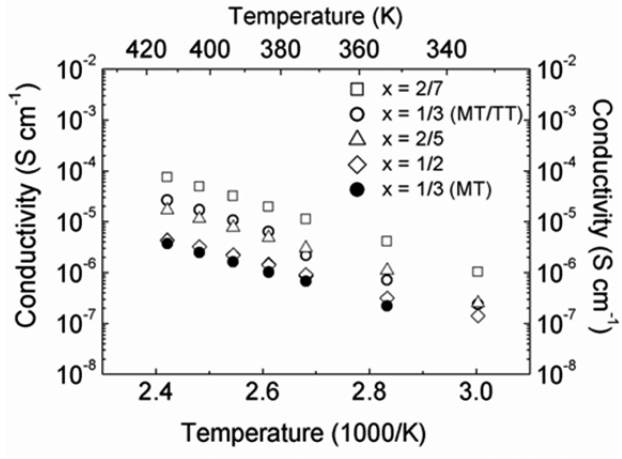

Figure 4. Plot of conductivity as a function of temperature for $Li(BH_4)_{(1-x)}Br_x$ on heating. All the materials shown were prepared by the combined mechanochemical and thermal treatment (MT/TT) except the $x = 0.333$ compound which was prepared by either MT/TT methods or by extended milling only MT.

ca. 10^{-6} S cm^{-1} at 313 K, 2 orders of magnitude higher than the orthorhombic phase of $LiBH_4$.[23] At 413 K the lithium ionic conductivity is ca. 10^{-4} S cm^{-1}. The activation energies for these materials vary in the range 0.52(2)−0.64(1) eV (Table S2). The $x = 0.333$ material was prepared both by extended milling and by milling/thermal routes. The latter method notably led to a higher value of conductivity.

The method of synthesis has a clear impact on the total resistance of these samples. The $Li(BH_4)_{0.667}Br_{0.333}$ sample prepared exclusively by mechanochemical processing (MT) shows a conductivity that is ca. an order of magnitude lower than the sample of the same composition prepared by a mixture of mechanical and thermal treatments (MT/TT). The contribution of grain boundaries to the overall conductivity can be substantial, and the similar activation energy values indicate the same mechanism for charge transport is operative in both samples. There are extensive differences in particle sizes and morphology between these two samples, and this is therefore the probable cause of the variation in transport properties.

Structural Analysis. Although it was possible to identify the presence of single-phase samples of hexagonal material from the PXD data, they were unable to provide substantial insight into the structure of the phases due to the dominance of the X-ray scattering by the relatively heavy bromide ion. We therefore undertook powder neutron diffraction experiments in order to elucidate the structural chemistry that underpins the fast ionic conducting hexagonal phase further. For this purpose, a single composition, $Li(BH_4)_{0.667}Br_{0.333}$, was studied in detail as a function of temperature.

High quality PND data were collected from isotopically enriched $Li(BH_4)_{0.667}Br_{0.333}$ at room temperature. One existing structural model of the hexagonal phase of $LiBH_4$ comprises a fully ordered array of $(BH_4)^-$ tetrahedral anions and Li^+

DOI: 10.1021/acs.chemmater.5b03642
Chem. Mater. 2015, 27, 7780−7787

cations.[3] Our interpretation of the neutron diffraction data from $Li(BH_4)_{0.667}Br_{0.333}$ therefore began by attempting to fit this structural model to our data using a randomly disordered arrangement of bromide and $(BH_4)^-$ anions with Br and B occupying the same 2*b* site (2/3, 1/3, *z*; where $z \approx 0.2$) in the lattice. This failed to give a satisfactory fit to the data, and a Fourier search of the asymmetric unit showed a second scattering center close to that occupied by the boron and bromine atoms. Attempts to refine occupancies on both the sites simultaneously against neutron diffraction data alone were unsuccessful in producing a stable refinement. Therefore, laboratory X-ray diffraction data were incorporated into a multiple histogram refinement (Figure 5). This exploited the strong scattering of X-rays by the bromide anion to give an unambiguous and robust identification of the bromide position and site occupancy. From this point on, our analysis of structure proceeded simultaneously against neutron and X-ray diffraction data sets.

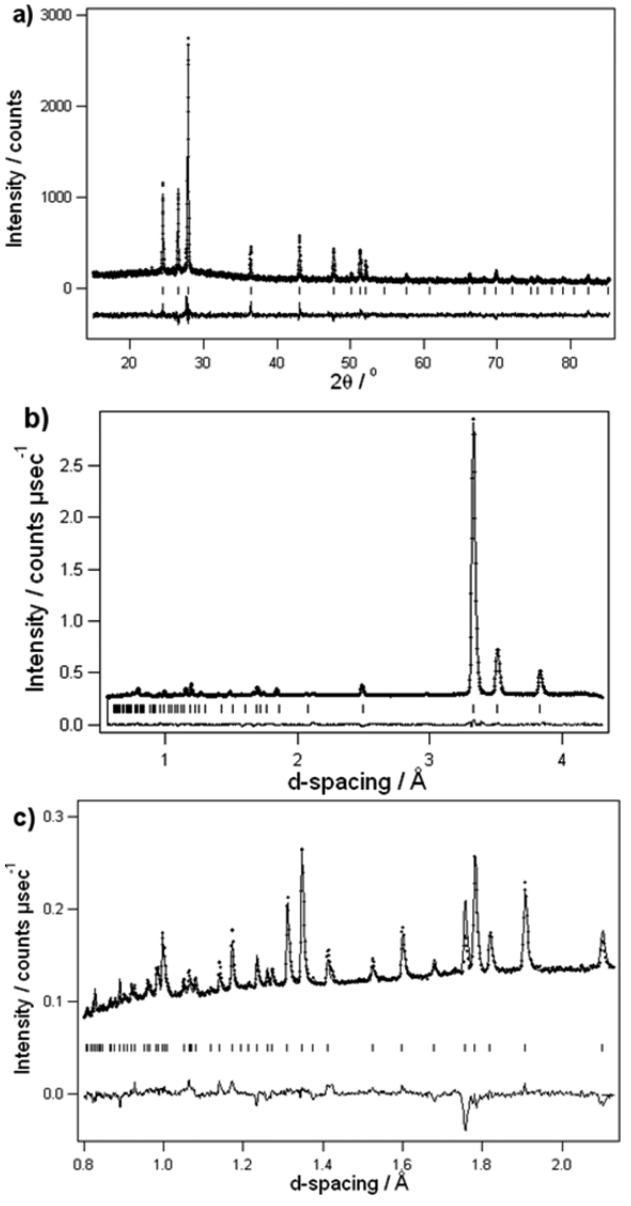

Figure 5. Rietveld profile fits for (a) PXD data and high-resolution neutron powder diffraction data collected from (b) bank 4 ($50° \leq 2\theta \leq 74°$) and (c) bank 5 ($79° \leq 2\theta \leq 106°$)[12] of the GEM diffractometer for $^7Li(^{11}BD_4)_{0.667}Br_{0.333}$ at 293 K. In each case, observed data are shown as dots, the calculated pattern as a solid line, and the difference profile as a solid line at the bottom of the plot. Vertical bars represent the reflection positions for the phase.

The deuterium atoms were initially assumed to be located on the vertices of a distorted boron-centered tetrahedron with one crystallographically unique atom and the other three related by a threefold rotation about the *z* direction.[7] No constraint was imposed on the ratio of BH_4^- to bromide; the refinement was able to proceed freely to select the anion ratio which best modeled the data. The ratio was fixed once the refinement was stable. With the deuterium atoms thus placed and their fractional occupancies constrained to be consistent with that of the boron atom to maintain the BD_4 stoichiometry, the structure was again refined and a Fourier map used to identify deficiencies in the model. This map showed positive scattering density to be present around the crystallographically unique deuterium atom occupying the 2*b* site, (2/3, 1/3, *z*; with $z \approx 0.4$) and thus suggested that the deuterium arrangement around the boron anion was heavily positionally disordered in a manner which can be described as a pseudoreflection in the *xy* plane containing the boron atom. The deuterium atoms in the complex anion were distributed around a single boron atom in a manner yielding two distorted tetrahedra; one tetrahedron aligned with an apical B−H bond parallel to the *c*-axis pointing "up" and conversely one aligned diametrically oppositely (pointing "down"). Attempts to construct a model with two separate boron centers were unsuccessful with the discrete boron atoms converging to one position. The overall fractional occupancy of the deuterium atoms was fixed such that the atoms refined as part of one of the tetrahedral units and the total deuterium content matched the stoichiometry demanded by the $(BH_4)^-$ anions.

Attempted refinement of anisotropic displacement parameters revealed an exceptionally elongated scattering center manifested by Li^+.[2] Due to the extreme nonphysicality of this distribution we elected to refine the lithium in an isotropic manner. In order to mimic the anisotropic scattering two lithium sites were introduced leading to a stable refinement.[12,24] The thermal displacement parameters of the boron and bromine atoms were constrained to the same single value, and likewise all the deuterium and lithium atoms were required to take the same U_{iso} value, respectively. We note that the space group $P6_3mc$ is noncentrosymmetric and so it is necessary to define the *z* coordinate of one of the atoms in the structural model in order to fix the origin for the *c*-parameter (Figure 6).

Further neutron diffraction data sets were rapidly collected on heating up to 573 K. The count statistics of these data are poorer as a consequence of the procedure, and so full structural refinement was not attempted. Nevertheless, the same structural model gave good fits to these data and showed a linear evolution in the lattice parameter with temperature (Figure 7), indicative of a straightforward thermal expansion with no anomalous structural effects.

An additional data set was collected at 393 K with the same counting statistics as the room temperature data.

Again these data could be fitted in a similar manner, although it is noteworthy that it was not possible to obtain a stable refinement if the positions of all the deuterium atoms were allowed to vary simultaneously.

DOI: 10.1021/acs.chemmater.5b03642
Chem. Mater. 2015, 27, 7780−7787

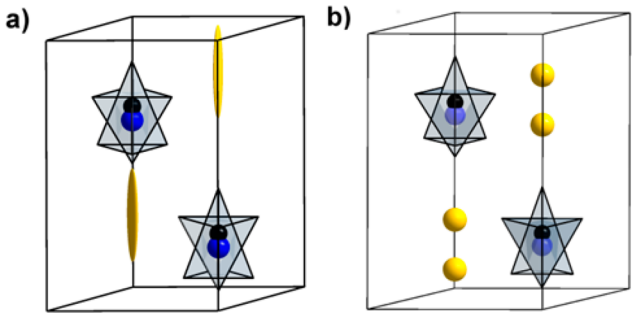

Figure 6. Crystal structure models of $^{7}Li(^{11}BD_4)_{0.667}Br_{0.333}$ with a polyhedral representation of the BD_4^- anion and showing (a) a single Li site with displacement parameters refined anisotropically and (b) two partially occupied Li positions with isotropic displacement parameters (D atoms are omitted; ellipsoids at 50% probability level).

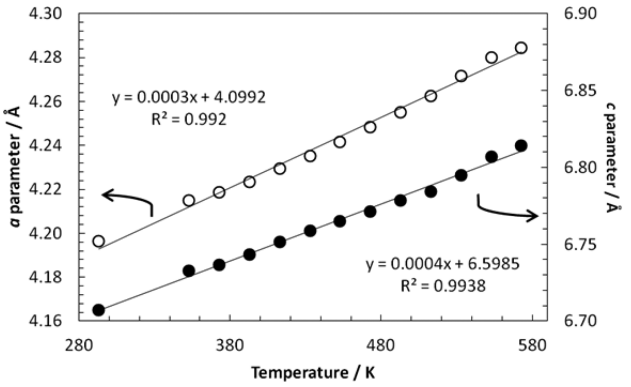

Figure 7. Cell dimensions of $^{7}Li(^{11}BD_4)_{0.667}Br_{0.333}$ as a function of temperature.

Inspection of the patterns collected at 393 K show a considerable reduction in the overall Bragg scattering intensities.

This would suggest further that at higher temperatures the structure displays an even higher level of disorder consistent with motion of the complex anions and diffusion of the lithium cations (as manifested in the thermal displacement parameters, for example).

Discussion. Reaction between lithium borohydride and lithium bromide can be driven stoichiometrically either by mechanically grinding materials together for 24 h or more readily by a 4 h mechanical treatment followed by heating at 573 K. PXD analysis before and after the TG-DTA examination of the heating stage of the MT/TT synthesis procedure (for example, for $Li(BH_4)_{0.667}Br_{0.333}$ as discussed above) shows that the initial 4 h grinding process causes a partial reaction between the LiBr and $LiBH_4$ to give a combination of an almost inappreciable quantity of the orthorhombic (LT-$LiBH_4$-type) phase and mostly a hexagonal (HT-$LiBH_4$-type) and cubic (LiBr-type) phase. That the temperature of the endothermic transition from the orthorhombic to hexagonal phase is reduced gives a strong indication that some degree of bromide incorporation into the hexagonal lattice has occurred during 4 h of MT. PXD evidence corroborates this premise. Both a steady decrease in the proportion of the LiBr-phase and a reduction in the cell parameters of the hexagonal phase can be observed on increasing the milling duration or as a result of subsequent heating. The process can thus be completed to give a single phase material either by further extended grinding (14 h) or by heating to 573 K after initial milling. Although we used intermittent grinding and rest periods to try and avoid excessive heat generation due to mechanical friction, we note that ball milling is often associated with very significant localized temperatures.[25] The degree of heating will of course depend on the heat capacities of the reagents and products involved as well as the coefficients of friction, hardness, and toughness, but it should be noted that the relatively modest temperature of 573 K necessary to afford a chemical reaction thermally is significantly lower than might be achieved by milling. For example, in the case of $La_7Mo_7O_{30}$, ball milling affords a phase which would otherwise only be stabilized by heating at temperatures above 1033 K.[26]

Although powder X-ray diffraction results indicate that the materials produced by either mixed mechanochemical/thermal or extended mechanochemical treatments are identical, their morphologies differ very substantially. The mechanochemical/thermal treatment affords regularly shaped particles of broadly cubic symmetry measuring approximately 1 μm across. Extended mechanochemical treatment, however, gives larger particles which appear to be aggregated into spheres around a central point. The observations of these petal-like structures have been made in other chemical systems where the presence of solvent is an essential condition to achieve flower-like growth.[27] Although the reaction described herein is between two solids to afford a solid final product, it should be noted that a eutectic mixture could readily form between the reagents. The localized heating during milling may deliver a sufficient quantity of liquid phase to initiate a mechanism of growth analogous to that seen in solution phase chemistry (the melting points of $LiBH_4$ and LiBr are 541 and 823 K, respectively).[22]

Syntheses and X-ray diffraction analysis have provided a structure−composition map for the $LiBH_4$−LiBr system. The end members of the system are orthorhombic and face-centered cubic, respectively, whereas our data demonstrate that intermediate compositions crystallize with the hexagonal structure of the HT phase of $LiBH_4$. Two-phase regions have been identified close to the orthorhombic-hexagonal and hexagonal-cubic phase boundaries (i.e., regions II and IV). It should be noted that adjustment of the heating conditions and cooling rates may be able to slightly increase the compositional limits of the single phases. Nevertheless our data show a number of interesting points in this compositional system which has hitherto been underappreciated.

Significant incorporation of the bromide anion into the $LiBH_4$ structure can be achieved within the orthorhombic structure. This substantial solubility means that it is necessary to introduce ca. 25% bromide into the structure before the hexagonal polymorph is stabilized at room temperature as a single phase. This hexagonal structure is stable for a wide range of anion compositions; a single phase exists from $0.29 \leq x \leq 0.50$. Interestingly, however, although a threshold value of bromide substitution is required to stabilize the higher Li ion conducting HT phase, beyond this composition point subsequent bromide substitution only serves to reduce the ionic conductivity. One can assume that this is associated with the concomitant contraction of the hexagonal unit cell and a less open migration pathway for Li^+ ions to diffuse.

For higher bromide concentrations the face centered (NaCl-type) cubic structure familiar from the LiBr phase is present in growing quantities as x increases. The variation in lattice parameters of the cubic phase for different reaction compositions suggests that the cubic material is not present

DOI: 10.1021/acs.chemmater.5b03642
Chem. Mater. 2015, 27, 7780−7787

as a line phase of composition LiBr; the incorporation of borohydride into the *fcc* lattice appears to be non-negligible.

Detailed inspection of the lattice parameters shows that significant changes in the unit cell volume occur with anion content of the overall reaction mixture. Where we have two-phase mixtures it is not possible to assign compositions unambiguously to each of the two phases. Nevertheless, inspection of the unit cell volumes for various reaction mixtures shows smooth evolutions in the lattice parameters implying substantial dissolution of both anions into all three structures. For each of the three structures (orthorhombic, hexagonal, and cubic), incorporation of the bromide anion with a radius of 1.96 Å in place of the larger borohydride anion radius of 2.05 Å gives the anticipated reduction in the unit cell volume.[28]

The high symmetry unit cell of $Li(BD_4)_{0.667}Br_{0.333}$ contains considerable occupational and positional disorder. Similar disorder has been observed in the hexagonal phase of $LiBH_4$ itself, which is stable above 383 K.[7,29,30] Nonetheless, Rietveld refinement against the neutron data was able to identify a narrow distribution of B−D distances in $Li(BD_4)_{0.667}Br_{0.333}$ (1.147(5)−1.32(1) Å at 293 K). Our analysis of the mixed anion compound shows that the presence of Br^- and BH_4^- within the structure leads to lithium bromide distances of 2.45(1) Å and 2.55(1) Å. Consideration of the BH_4^- and Br^- species shows that the two anions are displaced up and down the *c*-axis from the normal plane containing the borohydride anions in HT-$LiBH_4$ to sites which are separated by 0.31(1) Å in the *z*-direction. This displacement is mainly exhibited by the BH_4^- units leading to B···Li separations of only 2.476(3) and 2.68(7) Å (see Tables S4−S10).

The best fits to the diffraction data were obtained when the lithium ions were distributed over two tetrahedral (2/3, 1/3, *z*) sites: the position with $z \approx 0.8$ and that with $z \approx 0.6$. The former position is the one that has been previously identified as occupied in the HT-$LiBH_4$ structure,[2,30,31] but in the model refined here, this 2*b* site is 80% occupied.[32,33] Interestingly, the location and distribution of the lithuim ions is almost identical to that of the cations in another Wurtzite-related compound, *β*-CuI.[34,35] The Cu^+ ions in *β*−CuI exhibit a complex diffusion mechanism involving movement of the cations through the edges of the surrounding tetrahedral "cages" formed by I^-.[36] The structural similarities suggest that the disorder and diffusion of the Li^+ and Cu^+ ions in the respective borohydride and iodide fast ion conducting phases have a very similar origin. Nevertheless, the presence of complex ions in (HT-)Li-$(BH_4)_{1-x}Br_x$ necessitates anion orientations that facilitate the anticipated Li^+ diffusion process, given the observed high values of conductivity.

The orientation of the tetrahedral BH_4^- units is of crucial interest in understanding the lithium ion mobility through the structure. Considerable effort has been expended on examining the ionic transport behavior of undoped $LiBH_4$, although due to the presence of disorder and the challenges of identifying hydrogen atom positions there remains a considerable degree of uncertainty in this.[2,7,8] Our data could only be satisfactorily modeled by incorporating a distribution of deuterium atoms such that the tetrahedra were composed of two units centered on the same boron atom but with an inverted deuterium distribution. Although there is significant scatter in the B−D distances the observation of this inversion is robust and can be usefully compared with models of disorder that have been proposed from other techniques and calculations.[5,6,24] It should be noted that the understanding of the behavior of this anion is considerably complicated by the conflict between the trigonal symmetry of the crystallographic site and the tetrahedral symmetry expected for BH_4^-.

Various analyses have suggested that the dynamic disorder associated with the $(BH_4)^-$ anion arises from rotation about the threefold molecular axis or by complete spherical motion of the atoms around the boron center.[2,8,21,27] Our data show that neither of these descriptors provides a complete picture. While there is disorder around the trigonal axis, the data clearly identify well-localized atoms and attempts to delocalize them to other positions to give a halo of scattering density degraded the quality of fit and refinements failed to stabilize. Likewise, it was necessary to introduce an inverted distribution of deuterium atoms, but again these refined to specific positions and did not exhibit the instability that would be expected if the atoms occupying the unconstrained *x*, *y*, *z* coordinates of the 6*c* general position were free to move around points on a spherical scattering surface. A previous detailed study of the Raman spectra of HT-$LiBH_4$ suggested two thermally activated reorientations of the $[BH_4]^-$ unit with both rotation about the trigonal axis and a higher energy exchange being accessible.[3] Any assignment must remain tentative, but our structural data are most compatible with such a model. It is important to point out that no restraints were placed on the anion symmetry during refinement (nor, for example, were rigid body constraints applied).

Diffraction data collected on heating the material show that the key features of the crystalline structure are retained up to at least 573 K. Due to the diminishing Bragg scattering (and increase in diffuse scattering) from the sample at elevated temperatures it was necessary to introduce additional constraints to the structural refinement and so it is not possible to assign the disorder with complete confidence to either thermal motion or the static effects introduced by occupational disorder in the Br^- and BH_4^- sublattice.[37] The interplay of static and dynamic disorder should become clearer with a detailed study of structure as a function of both temperature and composition within each of the phase regions in the $LiBH_4$−LiBr system.

CONCLUSIONS

The hexagonal phase of $LiBH_4$ has been stabilized and isolated at room temperature by anion substitution over a compositional range $Li(BH_4)_{1-x}Br_x$ ($0.29 \leq x \leq 0.50$). Fast lithium ion conductivity is retained in these phases, although the value of the total conductivity is reduced as the bromide content increases above $x = 2/7$. There is considerable disorder in both the position and orientation of the anions in this structure leading to highly anisotropic distribution of lithium scattering. The Br^- and BH_4^- anions are displaced by a distance of 0.31 Å from each other in the crystallographic model with the latter exhibiting orientational disorder which can only be satisfactorily modeled using an inversion of the deuterium atoms. This implies substantial rotation of the BH_4^- units although not the free spherical rotation which has been observed in other complex anion fast ion conductors. Analysis of the Bragg scattering up to 573 K shows that the material retains this structure, although the reduced intensity of the Bragg reflections does suggest increasing disorder (loss of long-range order) in the material with heating.

DOI: 10.1021/acs.chemmater.5b03642
Chem. Mater. 2015, 27, 7780−7787

■ ASSOCIATED CONTENT

Supporting Information

The Supporting Information is available free of charge on the ACS Publications website at DOI: 10.1021/acs.chemmater.5b03642.

A list of samples and preparative procedures, Raman spectra, PXD data, AC impedance plots, refinement data, and tables of bond lengths and angles (PDF)

■ AUTHOR INFORMATION

Corresponding Authors

*(E.J.C.) E-mail: edmund.cussen@strath.ac.uk.

*(D.H.G.) E-mail: duncan.gregory@glasgow.ac.uk.

Notes

The authors declare no competing financial interest.

■ ACKNOWLEDGMENTS

The authors thank the University of Glasgow and University of Strathclyde for supporting this work and the Science and Technologies Facilities Council, UK, for the provision of neutron diffraction beam time.

■ ABBREVIATIONS

LT, orthorhombic phase; HT, hexagonal phase; MT, mechanochemical treatment; TT, thermal treatment

■ REFERENCES

(1) Matsuo, M.; Orimo, S. Lithium Fast-Ionic Conduction in Complex Hydrides: Review and Prospects. *Adv. Energy Mater.* **2011**, *1*, 161−172.

(2) Ikeshoji, T.; Tsuchida, E.; Ikeda, K.; Matsuo, M.; Li, H. W.; Kawazoe, Y.; Orimo, S. Diffuse and doubly split atom occupation in hexagonal $LiBH_4$. *Appl. Phys. Lett.* **2009**, *95*, 221901.

(3) Soulie, J. P.; Renaudin, G.; Cerny, R.; Yvon, K. Lithium boro-hydride $LiBH_4$. *J. Alloys Compd.* **2002**, *346*, 200−205.

(4) Filinchuk, Y.; Chernyshov, D.; Cerny, R. Lightest borohydride probed by synchrotron X-ray diffraction: Experiment calls for a new theoretical revision. *J. Phys. Chem. C* **2008**, *112*, 10579−10584.

(5) Hempelmann, R. *Quasielastic Neutron Scattering and Solid State Diffusion*; Oxford University Press: New York, 2000.

(6) Bée, M. *Quasielastic Neutron Scattering*; Adam Hilger: Bristol, 1988.

(7) Verdal, N.; Udovic, T. J.; Rush, J. J. The Nature of BH_4-Reorientations in Hexagonal $LiBH_4$ (vol 116, pg 1614, 2012). *J. Phys. Chem. C* **2012**, *116*, 5275−5275.

(8) Ikeshoji, T.; Tsuchida, E.; Morishita, T.; Ikeda, K.; Matsuo, M.; Kawazoe, Y.; Orimo, S. Fast-ionic conductivity of Li^+ in $LiBH_4$. *Phys. Rev. B: Condens. Matter Mater. Phys.* **2011**, *83*, 144301.

(9) Martelli, P.; Remhof, A.; Borgschulte, A.; Ackermann, R.; Strassle, T.; Embs, J. P.; Ernst, M.; Matsuo, M.; Orimo, S. I.; Zuttel, A. Rotational Motion in $LiBH_4$/LiI Solid Solutions. *J. Phys. Chem. A* **2011**, *115*, 5329−5334.

(10) Rude, L. H.; Groppo, E.; Arnbjerg, L. M.; Ravnsbaek, D. B.; Malmkjaer, R. A.; Filinchuk, Y.; Baricco, M.; Besenbacher, F.; Jensen, T. R. Iodide substitution in lithium borohydride, $LiBH_4$-LiI. *J. Alloys Compd.* **2011**, *509*, 8299−8305.

(11) Rude, L. H.; Nielsen, T. K.; Ravnsbaek, D. B.; Bosenberg, U.; Ley, M. B.; Richter, B.; Arnbjerg, L. M.; Dornheim, M.; Filinchuk, Y.; Besenbacher, F.; Jensen, T. R. Tailoring properties of borohydrides for hydrogen storage: A review. *Phys. Status Solidi A* **2011**, *208*, 1754−1773.

(12) Hannon, A. C. Results on disordered materials from the GEneral Materials diffractometer, GEM, at ISIS. *Nucl. Instrum. Methods Phys. Res., Sect. A* **2005**, *551*, 88−107.

(13) Larson, A. C.; Von Dreele, R. B. *General Structure Analysis System (GSAS)*; Los Alamos National Laboratory Report LAUR 86-748; Los Alamos National Laboratory: 1994.

(14) Toby, B. H. EXPGUI, a graphical user interface for GSAS. *J. Appl. Crystallogr.* **2001**, *34*, 210−213.

(15) Maekawa, H.; Matsuo, M.; Takamura, H.; Ando, M.; Noda, Y.; Karahashi, T.; Orimo, S. I. Halide-Stabilized $LiBH_4$, a Room-Temperature Lithium Fast-Ion Conductor. *J. Am. Chem. Soc.* **2009**, *131*, 894−895.

(16) Sveinbjornsson, D.; Myrdal, J. S. G.; Blanchard, D.; Bentzen, J. J.; Hirata, T.; Mogensen, M. B.; Norby, P.; Orimo, S. I.; Vegge, T. Effect of Heat Treatment on the Lithium Ion Conduction of the $LiBH_4$-LiI Solid Solution. *J. Phys. Chem. C* **2013**, *117*, 3249−3257.

(17) Miyazaki, R.; Karahashi, T.; Kumatani, N.; Noda, Y.; Ando, M.; Takamura, H.; Matsuo, M.; Orimo, S.; Maekawa, H. Room temperature lithium fast-ion conduction and phase relationship of LiI stabilized $LiBH_4$. *Solid State Ionics* **2011**, *192*, 143−147.

(18) Hartman, M. R.; Rush, J. J.; Udovic, T. J.; Bowman, R. C.; Hwang, S. J. Structure and vibrational dynamics of isotopically labeled lithium borohydride using neutron diffraction and spectroscopy. *J. Solid State Chem.* **2007**, *180*, 1298−1305.

(19) Orimo, S.; Nakamori, Y.; Zuttel, A. Material properties of MBH_4 (M= Li, Na, and K). *Mater. Sci. Eng., B* **2004**, *108*, 51−53.

(20) Gomes, S.; Hagemann, H.; Yvon, K. Lithium boro-hydride $LiBH_4$ II. Raman spectroscopy. *J. Alloys Compd.* **2002**, *346*, 206−210.

(21) Mosegaard, L.; Møller, B.; Jorgensen, J. E.; Bosenberg, U.; Dornheim, M.; Hanson, J. C.; Cerenius, Y.; Walker, G.; Jakobsen, H. J.; Besenbacher, F.; Jensen, T. R. Intermediate phases observed during decomposition of $LiBH_4$. *J. Alloys Compd.* **2007**, *446*, 301−305.

(22) Haynes, W. M.; Bruno, T. J. *CRC Handbook of Chemistry and Physics*, 95th ed.; CRC Press: 2014−2015.

(23) Matsuo, M.; Nakamori, Y.; Orimo, S.; Maekawa, H.; Takamura, H. Lithium superionic conduction in lithium borohydride accompanied by structural transition. *Appl. Phys. Lett.* **2007**, *91*, 224103.

(24) Renaudin, G.; Gomes, S.; Hagemann, H.; Keller, L.; Yvon, K. Structural and spectroscopic studies on the alkali borohydrides MBH_4 (M = Na, K, Rb, Cs). *J. Alloys Compd.* **2004**, *375*, 98−106.

(25) James, S. L.; Adams, C. J.; Bolm, C.; Braga, D.; Collier, P.; Friscic, T.; Grepioni, F.; Harris, K. D. M.; Hyett, G.; Jones, W.; Krebs, A.; Mack, J.; Maini, L.; Orpen, A. G.; Parkin, I. P.; Shearouse, W. C.; Steed, J. W.; Waddell, D. C. Mechanochemistry: opportunities for new and cleaner synthesis. *Chem. Soc. Rev.* **2012**, *41*, 413−447.

(26) Goutenoire, F.; Retoux, R.; Suard, E.; Lacorre, P. Ab initio determination of the novel perovskite-related structure of $La_7Mo_7O_{30}$ from powder diffraction. *J. Solid State Chem.* **1999**, *142*, 228−235.

(27) Benjacob, E.; Garik, P. The formation of patterns in noneequilibrium growth. *Nature* **1990**, *343* (6258), 523−530.

(28) Housecroft, C. E.; Sharpe, A. G. *Inorganic Chemistry*, 1st ed.; Peason Education: Harlow, Essex, U.K., 2001.

(29) Buchter, F.; Lodziana, Z.; Mauron, P.; Remhof, A.; Friedrichs, O.; Borgschulte, A.; Zuttel, A.; Sheptyakov, D.; Strassle, T.; Ramirez-Cuesta, A. J. Dynamical properties and temperature induced molecular disordering of $LiBH_4$ and $LiBD_4$. *Phys. Rev. B: Condens. Matter Mater. Phys.* **2008**, *78*, 094302.

(30) Remhof, A.; Lodziana, Z.; Martelli, P.; Friedrichs, O.; Zuttel, A.; Skripov, A. V.; Embs, J. P.; Strassle, T. Rotational motion of BH_4 units in MBH_4 (M = Li,Na,K) from quasielastic neutron scattering and density functional calculations. *Phys. Rev. B: Condens. Matter Mater. Phys.* **2010**, *81*, 214304.

(31) Remhof, A.; Yan, Y. G.; Embs, J. P.; Sakai, V. G.; Nale, A.; de Jongh, P.; Lodziana, Z.; Zuttel, A. Rotational disorder in lithium borohydride. *EPJ Web Conf.* **2015**, *83*, 02014.

(32) Aeberhard, P. C.; Refson, K.; David, W. I. F. Molecular dynamics investigation of the disordered crystal structure of hexagonal $LiBH_4$. *Phys. Chem. Chem. Phys.* **2013**, *15*, 8081−8087.

(33) Aeberhard, P. C.; Williams, S. R.; Evans, D. J.; Refson, K.; David, W. I. F. Ab initio Nonequilibrium Molecular Dynamics in the Solid Superionic Conductor $LiBH_4$. *Phys. Rev. Lett.* **2012**, *108*, 095901.

DOI: 10.1021/acs.chemmater.5b03642
Chem. Mater. 2015, 27, 7780−7787

(34) Hull, S.; Keen, D. A. High-pressure polymophism of the copper (I) halides - a neutron-diffraction study to similar to 10 GPa. *Phys. Rev. B: Condens. Matter Mater. Phys.* **1994**, *50*, 5868−5885.
(35) Keen, D. A.; Hull, S. Determination of the structure of beta-CuI by high-resolution neutron powder diffraction. *J. Phys.: Condens. Matter* **1994**, *6*, 1637−1644.
(36) Zheng-Johansson, J. X. M.; McGreevy, R. L. A molecular dynamics study of ionic conduction in CuI 0.2. Local ionic motion and conduction mechanisms. *Solid State Ionics* **1996**, *83*, 35−48.
(37) Elliott, S. R. *Physics of amorphous materials*, 2nd ed.; Longman Scientific & Technical; J. Wiley: Harlow, Essex, England; New York, 1990.

DOI: 10.1021/acs.chemmater.5b03642
Chem. Mater. 2015, 27, 7780−7787